

Article

Synchronous Generator out of Step Detection Using Real Time Load Angle Data

Ivan Višić ¹, Ivan Strnad ^{2,*} and Ante Marušić ³

¹ Pro Integris Ltd, 21000 Split, Croatia; ivan.visic@prointegris.hr

² Pro Integris Ltd, 10000 Zagreb, Croatia

³ Department of Energy and Power Systems, University of Zagreb Faculty of Electrical Engineering and Computing, 10000 Zagreb, Croatia; ante.marusic@fer.hr

* Correspondence: ivan.strnad@prointegris.hr

Received: 27 April 2020; Accepted: 28 June 2020; Published: 30 June 2020

Abstract: Although the power system usually always appears stable and reliable to consumers, a lot of work and research goes into keeping the power system both stable and reliable under constantly changing conditions and in these increasingly demanding times. One of the key issues in the power system is maintaining stability after large disturbances in order to prevent the loss of synchronicity of the generators in the system. Today's generator protection systems mostly use measurements of impedance change to detect generator out of step. This article discusses the possibility of detecting the loss of synchronicity by using real time load angle measurements. The authors propose a real time load angle measurement algorithm and present the results of the algorithm's testing performed on a real hydrogenerator. The results show that the developed algorithm gives highly accurate real time load angle measurements with the maximum possible resolution and that the load angle can be used for detecting the synchronous generator out of step.

Keywords: synchronous generator; load angle; power system stability; air gap; loss of synchronicity; out of step generator protection

1. Introduction

Power system stability is crucial for normal, reliable and safe power system operation. System disturbances that lead to power system oscillations, such as short circuits, can harm synchronous generators but can also cause a part or the entire power system to black out. It is necessary to protect the power system and the generators from these faults which can cause considerable damage.

Power system stability is defined in literature as the ability to regain an equilibrium state after being subjected to a physical disturbance. The quantities important for power system operation are the load angles of generators and the load angles, frequency and voltages of the nodes in the network. Consequently, the stability is divided into rotor angle stability, frequency stability and voltage stability [1]. Generator loss of synchronicity phenomenon is related to the rotor angle stability and will be discussed in this article.

The generator protection device is one of the key parts of every power plant. It uses input parameters (measurements and signals) and built-in algorithms to protect the generator from faults in auxiliary generator systems, faults in the grid and internal generator faults. One of the functions with a leading role in generator protection is the out of step protection function, whose role is to detect the generator loss of synchronicity. When the loss of synchronicity occurs, like during important power line outages and short circuits, the asynchronous areas must be isolated before the generator is damaged and other outages start occurring all over the system. This happens because high amplitude currents cause strains in generator windings as well as mechanical strains that can lead to generator and turbine damages [2]. Generator faults caused by such malfunctions often bring

significant financial costs, like expensive repairs and revenue loss due to production interruptions, so it is important to detect the fault and shut down the turbine and generator as soon as possible [3]. The out of step protection function is mostly implemented by assessing the generator stability based on the monotony, continuity and uniformity of impedance change [4,5] in the protection relays. The disadvantage of the methods based on impedance measurement is that they require extensive transient stability studies which cannot easily cover all possible disturbances in the system. On the other hand, the generator load angle is a value that specifically indicates the position of the generator operating point in relation to the border of stable operation and it could be used for generator protection purposes [6]. One of the reasons why it is not often used is the complexity of its real time measurement [7]. The concept of the generator protection system with a separated out of step function which uses real time load angle measurements is described in [8,9].

Because this problem is quite specific, very little literature on the subject is available altogether, let alone new literature. The goals of the authors' research can be divided into several phases:

- Analysis and selection of the load angle measurement method
- Development of the real time load angle measurement algorithm
- Development of the loss of synchronicity detection algorithm based on the real time load angle measurement

The focus of this article is on the first two research phases, but some proposals are given, and the discussion is opened on the third research phase—loss of synchronicity detection algorithm. An overview of the power system stability problems and the existing methods for the detection of the loss of synchronicity are given in Section 2. The same chapter provides a definition of the load angle and the existing methods for measuring it. The real time load angle measurement algorithm, the testing environment for real time load angle measurement and the simulation model are shown in Section 3. Section 4 shows the main results of the real time load angle algorithm testing and the conducted loss of synchronicity simulation analyses. The analyses set out to answer the question if the load angle is a good enough indicator (or value) that can be used for detecting the generator loss of synchronicity, and whether it can be used for conducting the generator out of step protection function.

2. Power System Stability and Load Angle

2.1. Power System Stability

All generators in an interconnected power system are working with the same frequency and the rotor mechanical speed is synchronized to this frequency. In technical terminology it is said that the generators are “in step”. This electrical connection between synchronous generators is elastic and allows angle fluctuations between them. Following some disturbances like short circuits which lead to line losses, the rotors of some generators will start to oscillate. The ability of the generators in the power system to remain in synchronicity those oscillations is referred to as rotor angle stability [10]. If a short circuit occurs and before the protection trips, a balance between mechanical power applied on the turbine and electrical power delivered to the system exists on each generator. When the protection trip occurs, the load in the system is changed rapidly but the change of mechanical power on the prime mover is much slower. This produces differences between mechanical and electrical torque in generators, and thus the rotor angle changes. The simplified relationship between the power output on generators and the rotor angle positions of the synchronous generators is represented by the following equation:

$$P = \frac{E_g \cdot U_s}{X} \sin \delta \quad (1)$$

where E_g is induced generator voltage, U_s is voltage at generator terminals, X is generator reactance and δ is the angle between voltages or load angle. A graphical representation of this nonlinear equation is shown in Figure 1.

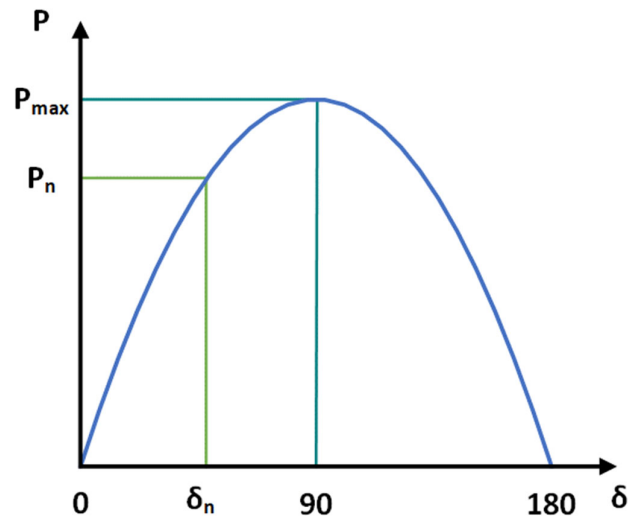


Figure 1. Load angle curve [11].

This is an idealized equation and representation, but it can be used to describe the system behavior. Therefore, in Figure 1 the transferred power rises with angle difference, but only to a certain point. The maximum transferred power is reached at an angle of 90° and any further increase in the angle will result in a decrease of transferred power. The power transferred at 90° is at its maximum under steady state conditions.

The same characteristic can be used to describe what happens during transient conditions. Initially, the system is in balance with transferred power P_n at the load angle of δ_n . After the protection trip occurs and the breaker is opened, the transferred power is reduced instantaneously and the mechanical power remains the same. Due to this difference, the rotor starts to accelerate and the angle δ increases. When the fault is cleared, the reached angle is δ_c but the rotor continues to accelerate since there is accumulated kinetic energy in it. At this point the rotor starts to decelerate since the electric torque is higher than the mechanical. The rotor decelerates till the angle δ_r is reached and all accumulated kinetic energy is used up. In Figures 1 and 2 it can be noticed that a critical angle δ_c exists, above which further increase in the angle results in lower electrical power and the generator starts to accelerate with no recovery. It can be concluded that the generator will maintain its stability if there is sufficient decelerating energy to oppose the acceleration. This is called the equal area criterion.

From the mentioned criterion it is also obvious that a critical time exists in which the fault must be cleared in order to maintain the stability of the generator. This time depends on the generator reactance and inertia constants. Since the size of the machines has increased and the inertia constants have decreased in the last decade, the critical times are reduced as well. If the loss of generator synchronicity occurs, high amplitude currents cause strains in generator windings as well as mechanical strains that can lead to generator and turbine damages. Therefore, it is important to clear the fault as soon as possible.

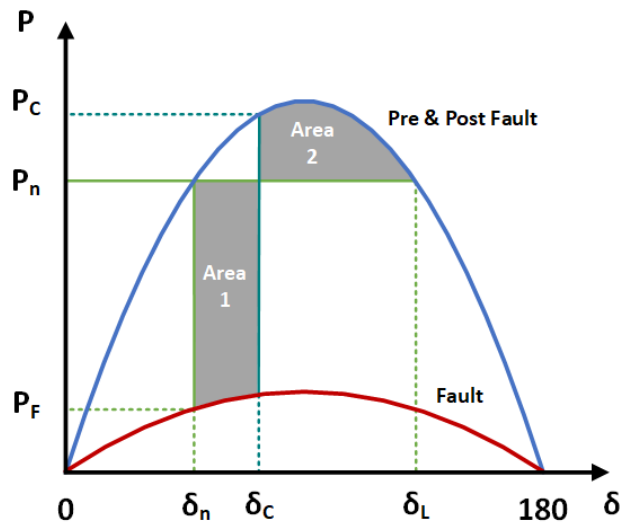


Figure 2. Power transmission capability of the normal system (blue curve) and the system with fault (red curve) [11].

2.2. Load Angle Definition and Measurement

Hydrogenerators and turbogenerators can be described by a distinctive standard two-axis mathematical model. In order to describe the synchronous generator with this mathematical model, the generator parameters have to be known. The load angle is one of the main synchronous generator parameters and the precise load angle measurement is imperative for determining the mathematical model. The load angle is mostly used in the generator monitoring systems, but its measurement in such systems is not conducted in real time [12]. The motivation behind this research was to evaluate if these measurements, conducted in real time, can be used for generator protection. Additionally, the load angle can be used for power system stability analysis and to determine losses of a generator. In these cases, the load angle must be measured in real time and in both static and transient generator operation modes.

The electrical load angle δ is the angle between induced EMF and terminal voltage or the angle between rotor and stator magnetic fields. The magnetic field of a synchronous generator rotates at synchronous speed and induces a rotating magnetic field in a stator but they are not completely aligned as the stator field lags behind the rotor field. This lagging is expressed in the load angle, as shown in Figure 3. The generated power is directly proportional to the sine value of this angle.

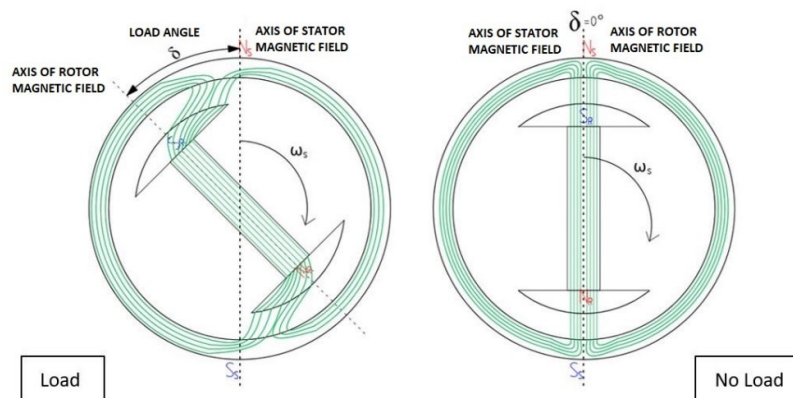


Figure 3. Graphical representation of the relation of rotor position, magnetic field and load angle.

When combined with the on-line capability chart (P-Q chart), the real time (on-line) measurement of the load angle (static and dynamic) is very important for determining the actual working parameters of a generator. Furthermore, the load angle is a key parameter in understanding torsional dynamics of a generator where magnetic field stiffness influences dynamic response of the generator.

As mentioned before, hydrogenerators and turbogenerators can be described by a distinctive standard two-axis mathematical model. The vector diagram in Figure 4 and Equations (2)–(5) [12] are based on the mentioned d_q mathematical model of the synchronous generator. In this representation the load angle is defined as the electrical angle between the space vector of the excitation voltage \bar{e}_q and the terminal voltage space vector \bar{v}_t . Since \bar{e}_q lies along the positive q axis, the load angle can also be defined as the electrical angle between the q axis and the voltage vector \bar{v}_t . At no-load condition \bar{e}_q and \bar{v}_t are identical and the load angle equals zero.

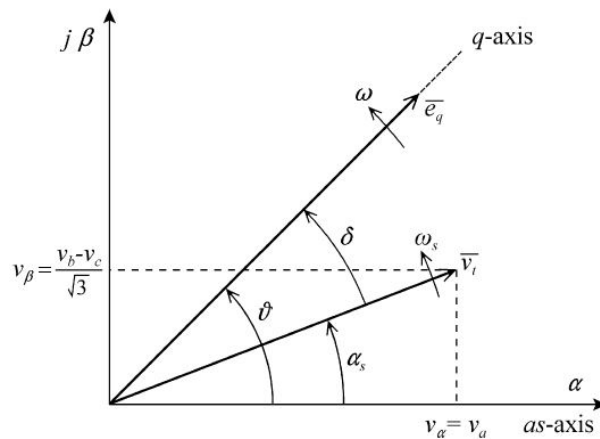


Figure 4. Vector diagram representing the definition of the load angle.

The resulting vector \bar{v}_t is defined in the stator coordination system $\alpha\beta$ where the real axis of this system corresponds to the phase of a winding axis as . When instantaneous values of generator terminal line voltages are known, the vector \bar{v}_t can be calculated from Equations (2) and (3). Based on this, the angle α_s which is the angle between vector \bar{v}_t and the axis as is defined in Equation (4) [12]:

$$\bar{v}_t = v_\alpha + jv_\beta = \sqrt{2}v_t e^{j\alpha_s} \quad (2)$$

$$v_t = \frac{1}{3} \sqrt{v_{ab}^2 + v_{bc}^2 + v_{ca}^2} \quad (3)$$

$$\alpha_s = \tan^{-1} \left(\frac{\sqrt{3}v_{bc}}{v_{ab} - v_{ca}} \right) \quad (4)$$

$$\delta = \vartheta - \alpha_s \quad (5)$$

Therefore, at symmetrical terminal voltage conditions the position of \bar{v}_t can be obtained by the phase angle of any line terminal voltage. The load angle can be obtained by measuring the rotor reference axis displacement referenced to the fundamental component of the line voltage, which is selected as the reference one, at load and no-load conditions respectively, as defined in Equation (5).

The load angle is determined by the terminal voltage signal of one phase and by the information on rotor position. Since the information on rotor position can be obtained in several different ways, different methods for determining the load angle also exist. The quality of the load angle measurements corresponds to the accuracy of determining the rotor position, and the rotor position

is usually determined in practice by different methods like the incremental encoder, inductive sensor and the capacitive air gap sensor.

The principle behind determining the rotor position by the inductive sensor is to use the inductive sensor for recording the passes of the gear teeth which are mounted on the generator shaft. The gear holds the same number of teeth as the pairs of poles, meaning that one impulse from the sensor appears in each period. An approximately sine signal is obtained at the output of the inductive sensor, and this signal is further modulated in frequency by the rotational speed of the rotor.

Measuring the load angle by using the incremental encoder is based on measuring the time difference between the reference marker and the incremental passage of the terminal voltage signal through zero-crossing.

The results shown in [12] suggest that the methods for determining the rotor position based on the incremental encoder and inductive sensor are very sensitive to vibrations and precession of the generator shaft. The capacitive air gap sensor method for determining the rotor position, or in other words for measuring the load angle, was developed to overcome these problems.

The capacitive air gap sensor measures the distance between the stator and rotor poles. The measurement of the distance between the stator and rotor poles is contactless and based on the capacitive flat-shaped probe which is mounted by simply being glued onto stator laminations. The capacitive air gap sensor for measuring the air gap width is in fact a measuring chain consisting of the probe and the linearization module (LM) [13,14]. An example of the capacitive air gap sensor is shown in Figure 5 [15]. The probe is connected to the linearization module via a triaxial cable and the linearization module sends a high frequency signal to the probe through the triaxial cable. The capacity is measured by a change in the phase of this signal, and the capacity directly depends on the air gap width. The linearization module is powered by DC voltage. On the output it produces a signal whose frequency is twice the grid frequency and is a good representation of the rotor position. After the signal is processed in the linearization module, a direct current output signal (4 to 20 mA) is obtained. This output signal is proportional to the generator air gap width. Figure 6 shows this signal u_{δ} recorded at a constant rotor speed and a sketch of the air gap width configuration [12]. The signal $u_{\delta 1}$ is a fundamental component of the u_{δ} signal and both signals are expressed in volts, while the angle ϑ is expressed in electrical radians. The load angle measurements require the air gap sensor signal to be tightly bound to the rotor position. If the rotor position correlates with the induced EMF, it can be used to determine the value of the load angle together with a terminal voltage signal. It can also be said that the phase shift of the capacitive air gap sensor signal towards the terminal voltage signal represents the load angle.



Figure 5. An example of a capacitive air gap sensor.

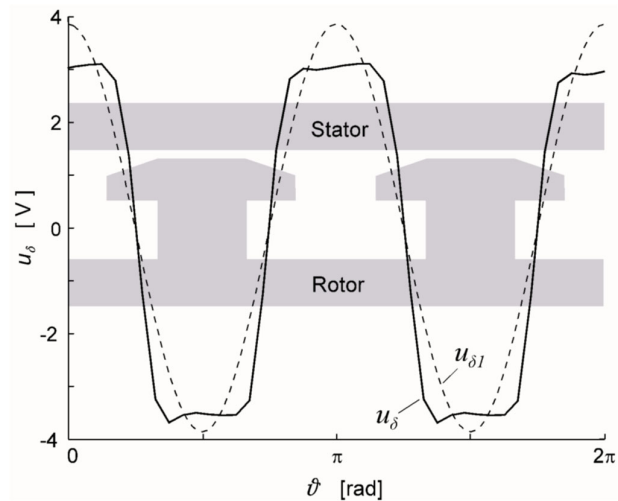


Figure 6. Signal from the air gap sensor after processing with regard to the rotor position.

Figure 7 shows the measurement results and the relationship between the terminal voltage signal and the capacitive air gap sensor signal. As the load angle increases, the air gap sensor signal starts leading in front of the voltage signal which is clearly shown in Figure 7. The blue curve represents the air gap sensor signal when the generator is excited but operates in the no-load mode. In this operation mode the active power and load angle values both equal zero. The green curve represents the air gap sensor signal when the generator is loaded and when the active power and load angle values are greater than zero.

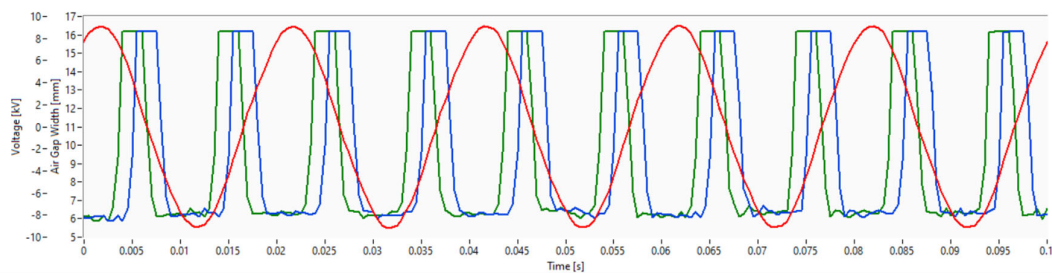


Figure 7. Relation of terminal voltage signal and air gap signal as load angle changes. The red curve represents the generator terminal voltage signal, the blue curve represents the air gap sensor signal when the generator is in the no-load operation mode and the green curve represents the air gap sensor signal when the generator is loaded.

When compared to the shaft encoder, the capacitive air gap sensor gives more stable and precise information on the rotor position because of the small radius of the shaft encoder ring compared to the rotor radius [16–19]. The research results shown in [12] confirm that the air gap sensor method for measuring the load angle is the most reliable, most precise and cheapest way of measuring the load angle. In the here presented research, the air gap sensor method is used for measuring the load angle.

Figure 8 confirms that this method gives stable results, as it shows the change of the load angle of the pumped-storage hydro unit under three operation modes: synchronous condenser, pumping and generator, with different active and reactive power. The measurements shown in Figure 8 were taken from the monitoring system of a pumped-storage hydro unit. Figure 8 shows the values of active power (red dots), reactive power (blue dots) and the load angle (green dots) over a period of 3 hours and 20 minutes. The interdependence of the load angle values and the active/reactive power values is clearly shown. In the period from 4:02 to 5:00 a.m. the pumped-storage hydro unit works

under the pumping (motor) operation mode, so the values of the load angle are negative. In the period from 5:00 to 5:45 a.m. the pumped-storage hydro unit works under the synchronous condenser operation mode (active power is 0 MW, and reactive power is about -75 MVar). Under this operation mode the load angle almost equals zero degrees because there is no load. At 5:45 a.m. the pumped-storage hydro unit is turned off and turned on again at 6:00 a.m. When the pumped-storage hydro unit is turned off and on, the load angle measurement loses its stability because the excitation is turned off. This instability is shown in Figure 8 in the time period between 5:45 and 6:00 a.m. After 6:00 a.m. the pumped-storage hydro unit works under the generator operation mode, where the load angle values are positive. At 7:00 a.m., when the active power increases, the load angle increases as well.

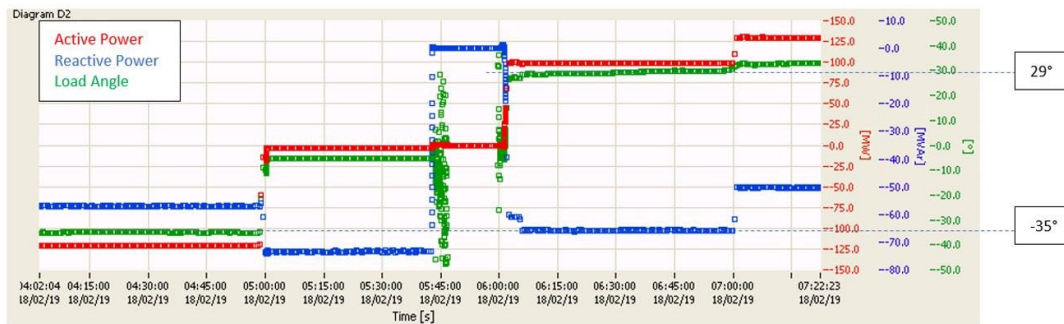


Figure 8. Change of load angle as active and reactive power change in time.

Measuring the load angle in real time is a relatively new procedure yet to be researched, and the full potential of this parameter of synchronous generator has not been used in practice. To date, it is most commonly used in generator monitoring systems. Different types of sensors are used for measuring the load angle, and because these measurements are very specific, one universal solution does not exist.

2.3. Loss of Synchronicity Detection Methods

A substantial amount of research has been conducted, as well as articles written, about the loss of synchronicity detection. The most commonly used detection method in today's numerical protection relays is based on the monitoring of impedance change at the generator terminals [20]. When using a simple example which consists of two systems A and B, their impedances Z_A and Z_B and the line impedance Z_L , then the impedance characteristic is presented in Figure 9.

If the voltages E_A and E_B are equal, i.e., $E_A/E_B = 1$ then the impedance characteristic is represented by the line PQ, and the angle between lines AP and BP is the load angle between the two systems δ . The line AB stands for total impedance. If system B is used as the reference system and it is assumed that E_A is leading E_B , then the impedance is changing from point A towards point B. During the loss of synchronicity, the impedance travels from point P to point Q. When the impedance intersects total impedance, the angle between two systems is 180° and it can be said that the systems are out of step. This point of intersection is known as the electrical center of the system. The impedance continues to travel and reaches again the point when the systems are in phase. At this point it is said that one out of step cycle has been completed. When the ratio E_A/E_B is not equal to 1, the impedance characteristics are represented by the curves as can be seen in Figure 9.

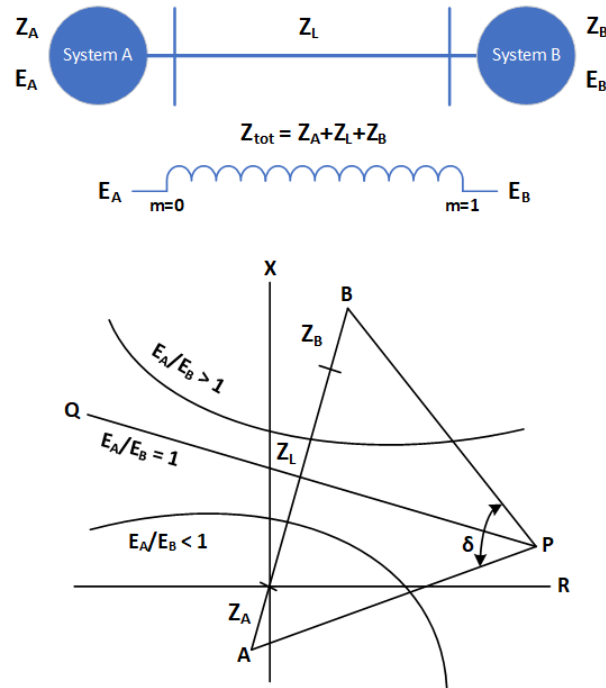


Figure 9. Impedance characteristic of the simple power system model.

The total impedance of the system consists of system A with impedance Z_A , line impedance Z_L and system B with impedance Z_B . The position of the loss of synchronicity protection relay is usually at the generator terminals and it divides total impedance into $m \cdot Z_{tot}$ and $(1 - m) \cdot Z_{tot}$ [21]. Impedance at the measurement location can be calculated by Equation (6):

$$Z(m) = \left[\frac{1}{1 - \frac{E_B}{E_A} \cdot e^{-j\delta}} - m \right] \cdot Z_{tot} \quad (6)$$

All methods for detecting the loss of synchronicity are based on impedance monitoring. There are several different implementations of this method, such as:

- Single blinder scheme
- Double blinder scheme
- Lens scheme
- Two zones scheme with straight lines

The common characteristic of these schemes is that they require extensive stability studies to determine loss of synchronicity characteristics, maximum generator slip, characteristic of stable swings and expected current levels in relays [3]. Because of this, there have been attempts of different researchers to propose some other methods to detect the out of step. The schemes can be divided into schemes that use only local measurement and the ones that use wide area measurement for decision-making. The authors in [22] are proposing a method that uses a change of rate of swing center voltage (SCV). This method does not require extensive analysis but uses some approximations for the calculation of SCV. The approach that combines time-domain analysis in Clarke's domain with the SCV method is presented in [23]. The algorithm that uses the well-known equal area criterion is presented in [24,25]. This method uses reactive power, real power, and the rate of change of real power to predict the out of step condition. Since the setting of the change of real power is based on the maximum slip, it requires extensive simulation studies [26]. Equal-Area Criterion combined with the least-squares method is used in [27]. The algorithm based on the same criterion but applied in the time domain is described in [28]. Reference [29] presents the R-Rdot algorithm that measures the

resistance at generator terminals, and the rate of change of this resistance to detect unstable swings. The disadvantage of this scheme is that it does not control the angle at which the tripping is issued. As the synchrophasor technology develops, some methods that use this technology are also being proposed [30]. For the methods using PMUs, communication and measurement equipment is needed at all relevant locations in the system. An interesting approach using wide-area measurements and generators' coherency identification in real time for system splitting decision is presented in [31]. The common characteristic of many of the methods used for the loss of synchronicity is the indirect prediction and/or detection of load angle behavior following disturbances in the power system.

Despite all of the newly proposed methods for the loss of synchronicity detection, the most commonly used algorithm in today's practice is still the detection of impedance change, as already mentioned at the beginning of this chapter. The impedance characteristic is presented in Figure 9 and the angle δ between lines AP and BP is the same angle that can be obtained by direct load angle measurement. In the impedance measurement method, the load angle change is supervised through the detection of impedance vector change and when this vector passes through the relay characteristic then the pole slip is detected. During the transient, the load angle changes from the start value (normally 30° to 40°), passes 180° and then comes back to the first value.

The dynamical behavior of the generator can be described by the following equations:

$$\frac{2H}{\omega_0} \frac{d^2\delta}{dt^2} = P_m - P_e \quad (7)$$

$$\frac{d\delta}{dt} = \omega \quad (8)$$

where H is the generator inertia constant and ω is the rated angular velocity. P_m and P_e are the mechanical input power and electrical output power respectively, δ is the load angle and ω is generator angular speed. From the equations and from what is stated in this chapter it can be concluded that if the load angle would be measured in real time, it could be used for generator loss of synchronicity protection purposes.

3. Materials and Methods

3.1. Real Time Load Angle Measurement Algorithm

A very precise and reliable measurement of the load angle must be provided in order to ensure its application for generator protection purposes, e.g., out of step protection function. The rest of this chapter will present the testing results and describe the method developed for measuring the direct load angle of the synchronous generator.

The load angle measurement algorithm functionalities include the air gap width measurement, generator voltage measurement, and rotor position detection. The main goal was to develop a method for measuring the load angle in real time which will provide a stable calculation or measurement of the load angle every 20 ms, i.e., after each period (for a 50 Hz system frequency). Because the load angle value is determined in the same way as the phasor value, this is the highest possible resolution in which it can be measured. When compared to the commonly used method for measuring the load angle shown in Section 2, this method takes into consideration the rotor imperfection. The rotor imperfection can be explained as a geometrical imperfection. This directly influences the precision of the air gap width measurement, and later the load angle value. The geometrical imperfection of the rotor is in fact structural in nature and is present in every generator. The imperfection is specific to every rotor and it is constant in time, meaning it is possible to correct the air gap width measurement for that specific imperfection. The above mentioned facts were all taken into consideration in the algorithm for measuring the load angle in real time.

The flowchart of the developed algorithm for measuring the load angle in real time is shown in Figure 10, and its main features will be briefly described in this section. In order to ensure the functioning of the algorithm, measurements of the air gap width, generator terminal voltage and keyphasor sensor signals have to be provided. For the basic algorithm functioning, only one air gap

sensor measurement and one generator terminal voltage measurement is enough, but this does not enable the algorithm's maximal measurement precision and quality. By using more than one air gap sensor measurement and three generator terminal voltage measurements (for each phase), the reliability of the measurements is significantly increased, without significantly increasing the costs of implementing such a system in comparison to the "one air gap sensor" system. After processing the input signals received from the air gap sensors and from the instrument transformers, the load angle is measured with the resolution of 20 ms or 50 values per second. The obtained values are the directly measured load angle values in real time that are very precise thanks to the developed algorithms or functions for signal processing and angle calculation.

To further improve the quality of the load angle measurements within the developed algorithm, a function for correcting the directly measured load angle values with respect to the rotor geometrical imperfection was added. To enable this functionality, both the correction data and the rotor position data must be accessible.

The characteristic of the imperfection, which depends on the rotor position, must be recorded in order to be applied in the load angle correction function. To be able to use this information in the algorithm, the rotor position must be determined first. This is easily done by using the signal from the keyphasor sensor which detects of one rotor turn. The correction data is determined in the calibrating process of the procedure for measuring the load angle in real time. The calibration of the load angle measurement system must be performed only once, during commissioning. The calibration has to be performed again in the cases when the generator undergoes specific maintenance or fault corrections that change the correction data, for example changing the position of the air gap sensor or mechanical interventions on the rotor that change the rotor geometry.

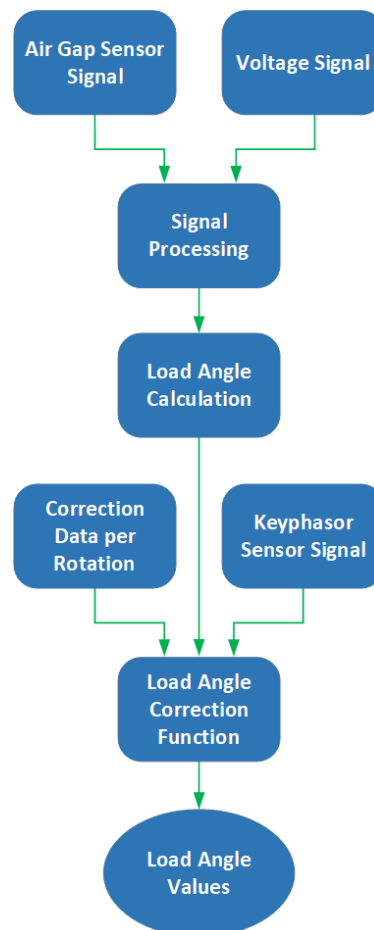


Figure 10. Flowchart of the developed real time load angle measurement algorithm.

3.2. Testing Environment for Real Time Load Angle Measurement

Figure 11 shows the testing environment developed for testing the above described real time load angle measurement algorithm. The testing environment includes the functions for the acquisition and processing of signals from sensors as well as the real time load angle measurement algorithm. It is based on the National Instruments (NI) hardware cRIO-9090 controller, the analog input module NI 9205 and the current output module NI 9266. The applications are developed in the systems engineering software LabVIEW. The testing environment acquires input signals through analog inputs, where three inputs are used for generator terminal voltages, three inputs for generator currents, three inputs for capacitive air gap sensor signals and one input for the keyphasor sensor signal. The technical specifications of the air gap sensor used in the tests are shown in Table 1. A/D conversion is performed with a sampling rate of 10 kHz for all analog inputs.

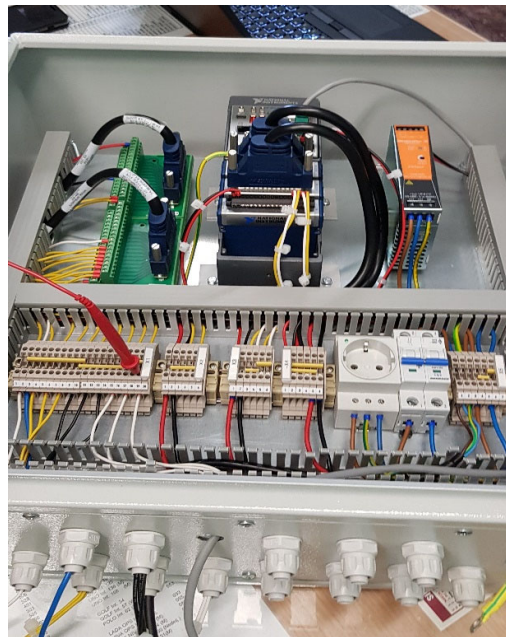


Figure 11. Testing environment for real time load angle measurement.

After the A/D conversion of the input signals, the acquired data is processed according to the steps of the algorithm shown in Figure 10. The real time load angle values are available through analog outputs or as digital data in the controller, accessible through the communication network to which the controller is connected.

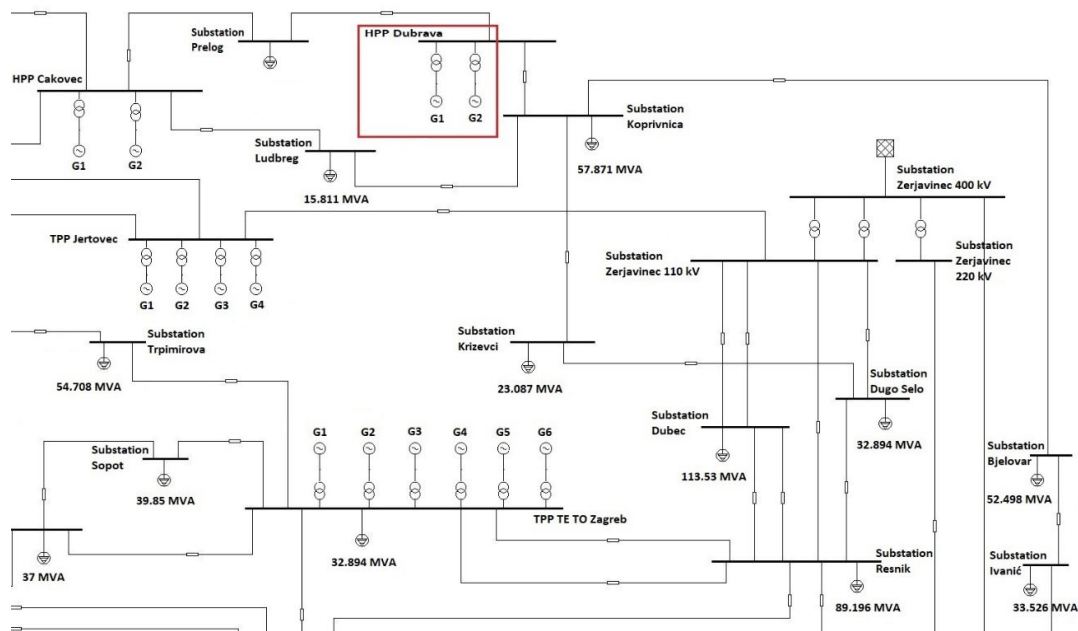
The functional testing of the real time load angle measurement algorithm in the real environment was conducted on a hydrogenerator of the Dubrava hydropower plant (HPP). Three capacitive air gap sensors and one keyphasor sensor are a part of the hydrogenerator's monitoring system. The signals from the sensors are connected to the cabinet of the monitoring system. Analog generator terminal voltages and generator current signals are also available in the same cabinet. Therefore, the testing environment was connected to the cabinet of the monitoring system where the analog signals from the air gap sensors, the keyphasor sensor and the terminal voltages and currents of the generator were all available. Because of this, the installation of the testing environment was performed quickly and easily. After the installation, a calibration procedure was performed under the generator no load operation mode and the correction data values were defined.

Table 1. Technical specifications of the capacitive air gap sensor Veski CGS020210 used in the testing.

Parameter	Unit	Value
Probe type		CGP-02
LM type		CGL0202
Probe dimension	mm	135 × 32 × 17
LM dimension	mm	125 × 80 × 60
Measuring range	mm	3 to 15
Power supply	VDC	18 to 36
Voltage output	VDC	2 to 10
Current output	mA	4 to 20
Operating temperature	°C	−15 to 70
Full range accuracy	%	±3

3.3. Loss of Synchronicity Simulation Model

The power system simulation software ETAP was used for analyzing the performance of the generator parameters with out of step and power swings. For this purpose, the northern part of the Croatian power system was modelled. For better visibility, only one part of the power system model is shown in Figure 12. The transmission system consists of 400, 220 and 110 kV lines and it is interconnected with Slovenian, Hungarian, Bosnian and Serbian power networks. In this part of the system there is one nuclear generator unit, several thermal and combined cycle units and 6 hydro units.

**Figure 12.** Illustration of a part of the Croatian power system topology used in the simulation.

Points of interest are the generators in the Dubrava HPP (marked in red in Figure 12) since they might be subjected to the loss of synchronicity. The main reason for that is because the generator rotors have very low mass and consequently a low inertia moment, although the problem is not so simple and different studies and articles have been written about power swings on the mentioned generators [32,33]. The main parameters of generators for the Dubrava HPP used in the simulations are presented in Table 2.

Table 2. Main parameters of generators in the Dubrava HPP.

Parameter	Symbol	Unit	Generator 1	Generator 2
Nominal power	S_n	MVA	42	42
Nominal active power	P_n	MW	39.9	39.9
Nominal voltage	U_{Gn}	kV	$6.3 \pm 7.5\%$	$6.3 \pm 7.5\%$
Power factor	$\cos\varphi_n$		0.95	0.95
Nominal speed	n	rpm	125	125
Nominal frequency	f_n	Hz	50	50
Inertia constant	T_A	s	1.05	1.05
Moment of inertia	$J(I)$	t m ²	1150	1150

Different power swings have been obtained and the behavior of the load angle, speed and other generator variables have been analyzed. The most severe situation concerning power swings of the generators is the three-phase fault on the power plant busbars, and this case was analyzed first. After that, the three-phase fault at the end of the lines going out from the Dubrava HPP was analyzed. Since the generators in the Dubrava HPP are identical, the behavior of only one generator was analyzed. It should be noted that all simulations were performed with constant excitation (no voltage regulation) and with no governor action during transient simulations.

4. Results

4.1. Testing Results of the Real Time Load Angle Measurement Algorithm

The above described testing environment was used for the functional testing of the real time load angle measurement algorithm under operating conditions of a real hydrogenerator. The results of the conducted tests are presented below.

Figures 13–15 show the algorithm testing results where the influence of the correction data on the load angle measurement is shown. Due to transparency, the results for only one rotor turn are given. Figure 13 shows the results of the load angle measurement when the load angle correction function is not applied. Figure 14 shows the results of determining the correction data in relation to the keyphasor signal sensor which were obtained in the process of algorithm testing. Figure 15 shows the results of the load angle measurement when the load angle correction function or correction data is applied. As shown in Figures 13–15, one rotor turn has 24 measured load angle values, so it should also contain 24 correction data values. Precisely 24 measured values per rotor turn result from the fact that one turn lasts 480 ms because the generator nominal speed equals 125 rpm, and the load angle measurement resolution is 20 ms. Since the correction data stands for the rotor geometrical imperfection, these values are always the same.

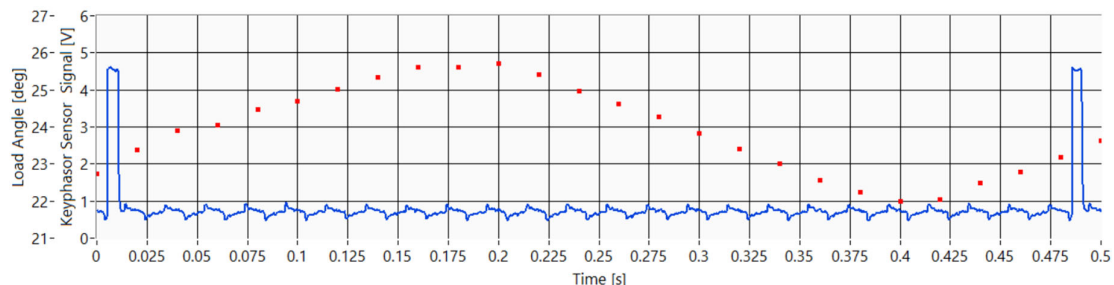


Figure 13. Results of the load angle measurement when the load angle correction function is not applied. The red dots represent the load angle values, and the blue curve the output of the keyphasor sensor.

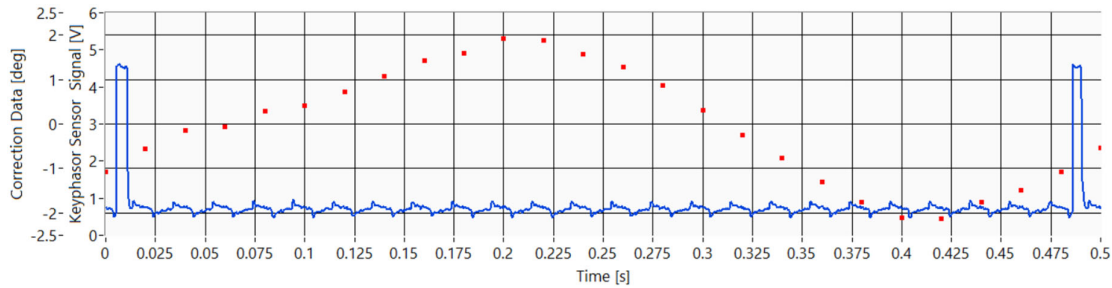


Figure 14. Results of determining the correction data in relation to the keyphasor sensor signal obtained in the algorithm testing. The red dots represent the correction data values.

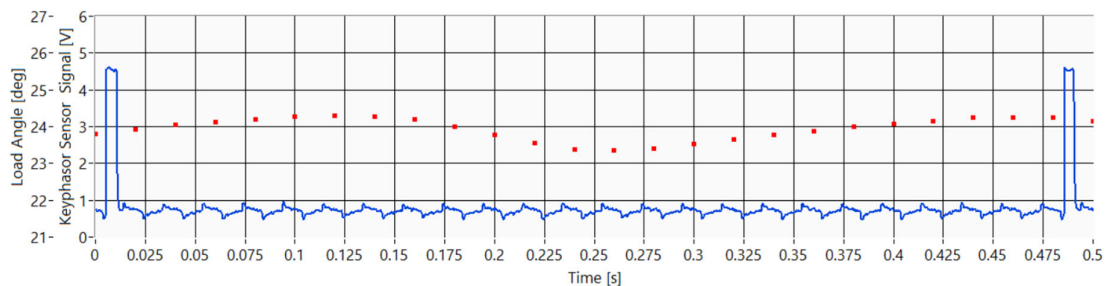


Figure 15. Results of the load angle measurement when the load angle correction function is applied. The red dots represent the corrected load angle values.

The results clearly show that correcting the rotor geometrical imperfection improves the stability and accuracy of the load angle measurement of the synchronous generator. The correction data differs from generator to generator and it is not possible to assess to what extent their application in the algorithm contributes to the improvement of the load angle measurements. Because these values are constant their influence is greater for smaller load angle values, and vice versa, the influence is smaller when the load angle values increase. The conducted analysis of the data obtained in the functional testing on a real hydrogenerator shows that, in this case, the usage of correction data in the algorithm increases the precision of the load angle measurement values (on average) by 5.4% compared to the values obtained when the correction function was not applied.

The testing results of the above described load angle measurement algorithm are shown next. Figure 16 shows the results of the load angle measurement of the synchronous generator under steady-state conditions. As it can be seen, the load angle measurement is in sync with the expected values, or in other words, there are no oscillations in the load angle values.

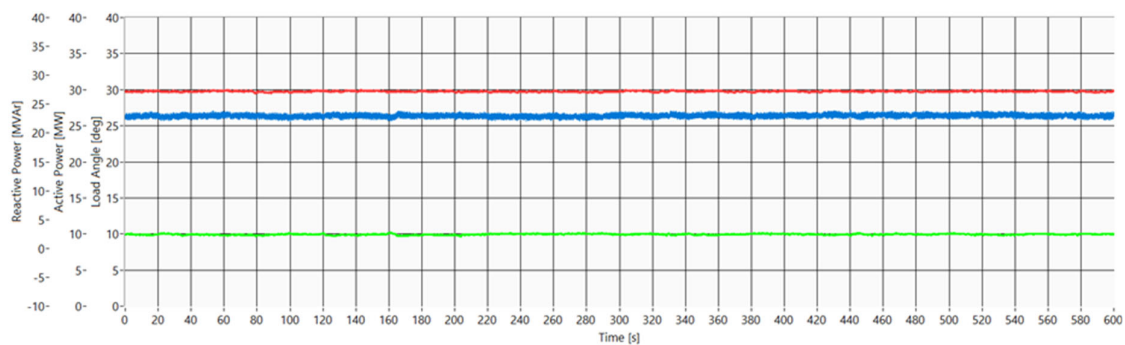


Figure 16. Testing results of the load angle measurement algorithm of the synchronous generator under steady-state conditions. The red curve represents the active power measurements, the green curve represents the reactive power measurements and the blue curve the load angle measurements.

Figure 17 shows the results of the load angle measurement under continuous change of the active power on the one hand, and constant reactive power on the other hand. The results show that the load angle curve follows the active power curve, pointing to the conclusion that the load angle measurement algorithm provides correct results. Figure 17 shows the example of starting a generator.

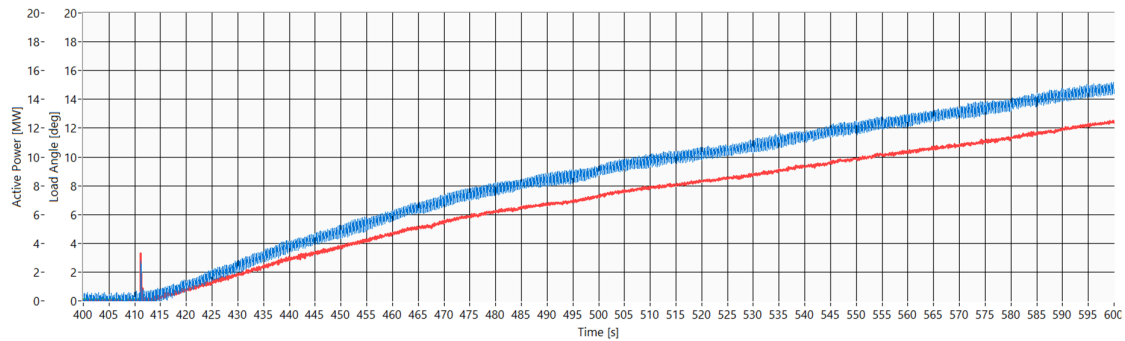


Figure 17. Testing results of the load angle measurement algorithm of the synchronous generator under continuous change of the active power. The red curve represents the active power measurements and the blue curve the load angle measurements.

To confirm the accuracy of the load angle measurement algorithm, additional tests where both active and reactive power are changed were conducted and their results are given in Figure 18. The results show that, in the case when reactive power is constant, the load angle curve follows the change in the active power curve, and this has already been confirmed in previous cases. This type of behavior is in line with the load angle definition. When the generator power swing fault occurs, the active power swings affect the load angle. The load angle values follow the changes in the active power. The results also show the behavior of the load angle when the reactive power is changed. This example depicts the change of reactive power of the generator, and the results show the response of the load angle to the change of reactive power. From the results of the conducted tests it can be seen that the increase of reactive power in the inductive region decreases the load angle, and vice versa. Furthermore, the load angle is bigger in the capacitive region than in the inductive region. When taking these two facts into account, it is evident that the generator stability is more subjected to instability in the capacitive region than in the inductive region. The algorithm testing results shown in Figure 18 directly confirm these postulates.

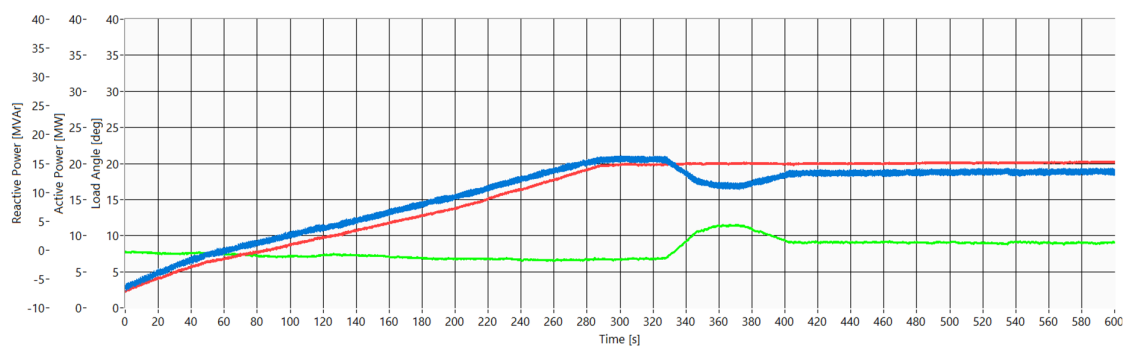


Figure 18. Testing results of the load angle measurement algorithm of the synchronous generator under a change in first the active and then the reactive power. The red curve represents the active power measurements, the green curve represents the reactive power measurements and the blue curve the load angle measurements.

4.2. Loss of Synchronicity Simulation Results

Figures 19–26 show the behavior of Generator 2 for the three-phase fault on the busbar at 100 ms and fault clearing at 270 ms from the start of the simulation. In the aforementioned Figures, the behavior of active power, reactive power, load angle and speed are presented. After the fault, the active power drops immediately and it is practically zero during fault time after which it jumps and then after some time stabilizes at the same power it had before the fault. At the same time the maximum load angle of 140° is reached at 300 ms from the start of the fault, and after that the angle starts to stabilize. The machine speed rises after fault, reaching the maximum at approximately 280 ms and then decelerates with oscillations.

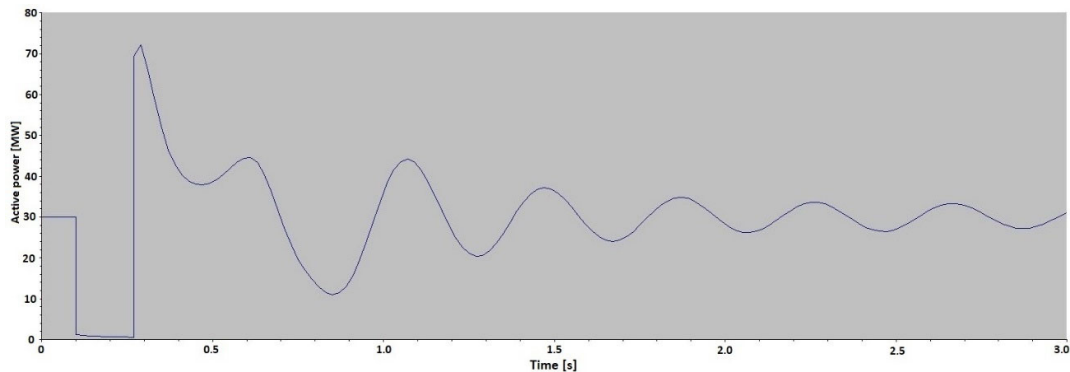


Figure 19. Simulation results of active power of Generator 2 during the three-phase fault with the fault duration of 170 ms.

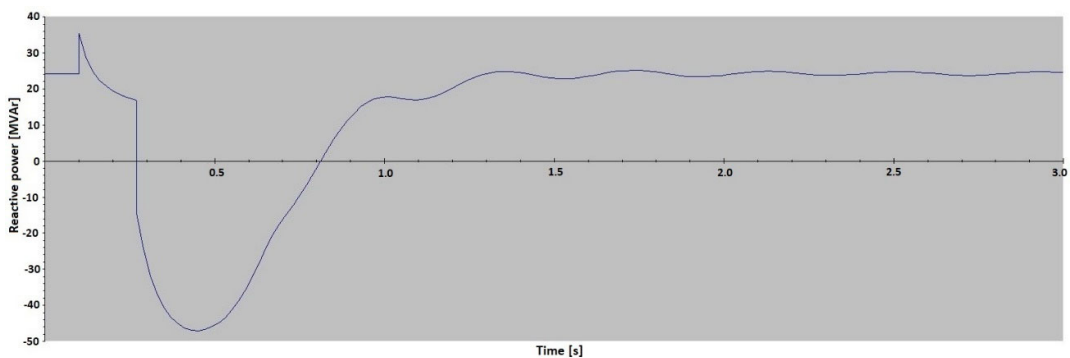


Figure 20. Simulation results of reactive power of Generator 2 during the three-phase fault with the fault duration of 170 ms.

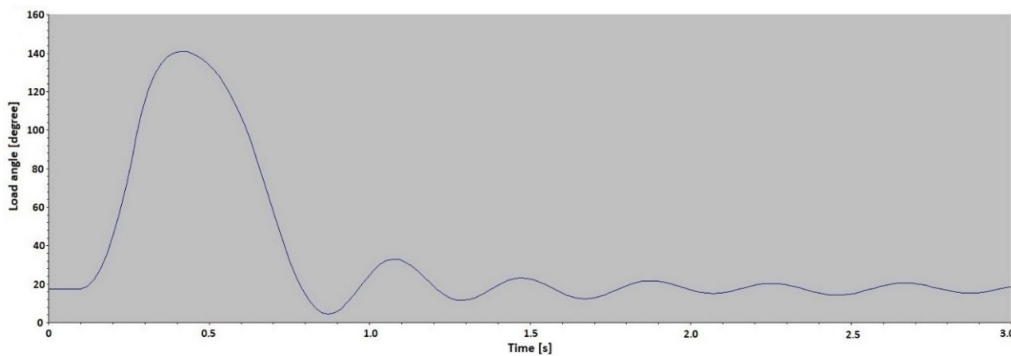


Figure 21. Simulation results of the load angle of Generator 2 during the three-phase fault with the fault duration of 170 ms.

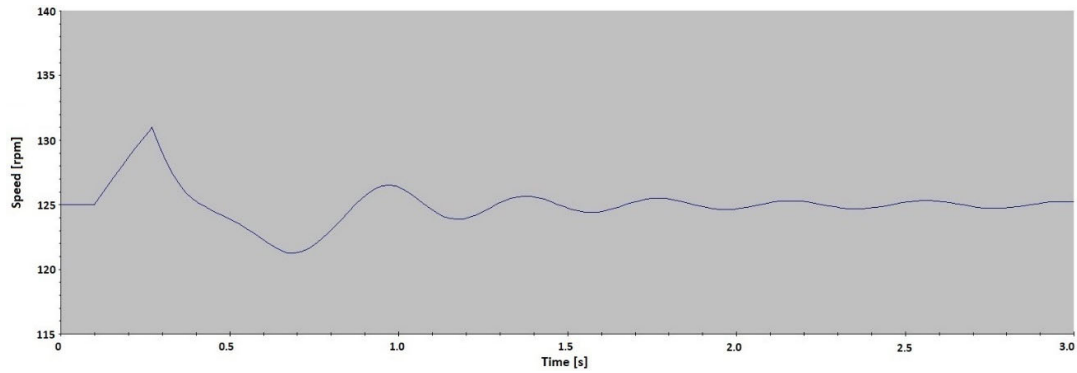


Figure 22. Simulation results of speed of Generator 2 during the three-phase fault with the fault duration of 170 ms.

For the fault with the duration of 172 ms, unstable power swings occur. The load angle is rising again but this time it does not stop at 140° but continues to rise and the generator goes out of step. The generator speed rises after the fault, but it does not decay like in the situation with a stable power swing. It continues to rise with oscillations. The value of 170 ms is the critical fault time for this generator for the fault at the busbars.

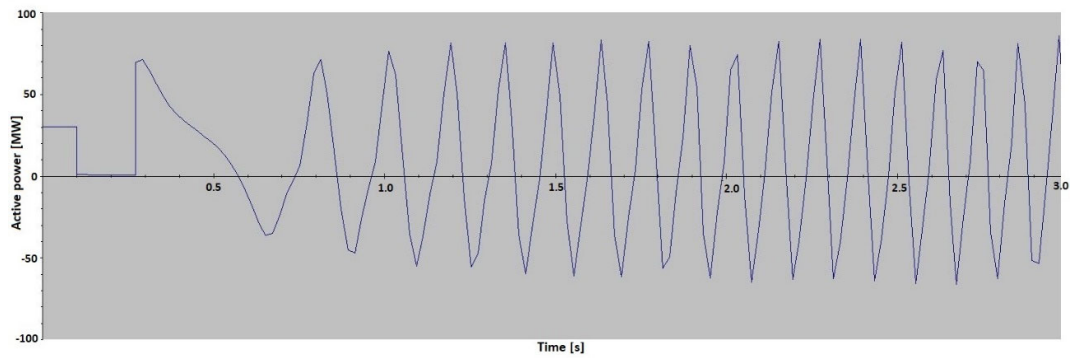


Figure 23. Simulation results of active power of Generator 2 during the three-phase fault with the fault duration of 172 ms.

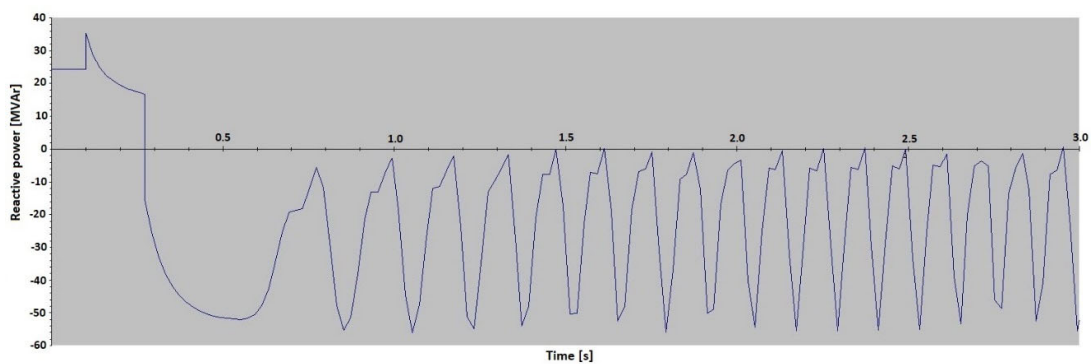


Figure 24. Simulation results of reactive power of Generator 2 during the three-phase fault with the fault duration of 172 ms.

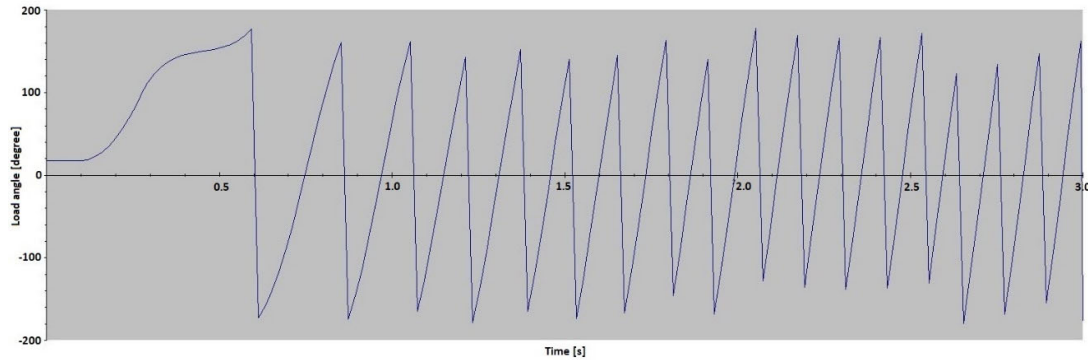


Figure 25. Simulation results of the load angle of Generator 2 during the three-phase fault with the fault duration of 172 ms.

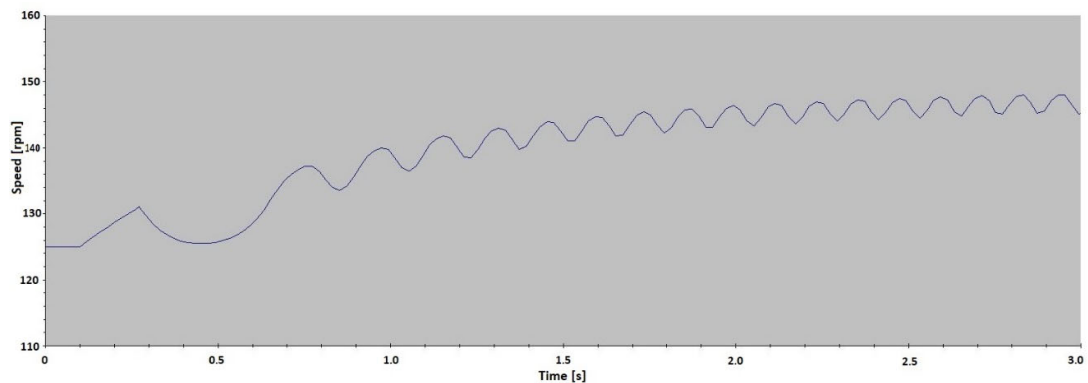


Figure 26. Simulation results of speed of Generator 2 during the three-phase fault with the fault duration of 172 ms.

The results of the simulation can be interpreted using equal area criterion already discussed in Section 2. After a short circuit happens, the active power is reduced immediately, and the generator starts to accelerate due to the difference between mechanical and electrical power. When the fault is cleared the active power reaches its previous value and the generator starts to decelerate. According to the simulation, 170 ms is the critical fault time for which the kinetic energy of accelerating (area 1 in Figure 2) is balanced with the kinetic energy of decelerating (area 2 in Figure 2). For longer fault times, the critical angle δ_L will be passed and further increase in the load angle will result in lower electrical power and the generator will start to accelerate with no recovery.

The simulations have been repeated for the three-phase faults at the end of the 110kV lines going out from the Dubrava HPP to the Prelog substation (SS) and Koprivnica SS. The critical fault time at the end of Prelog SS line (10.1 km) is 199 ms and at the end of the Koprivnica SS line (17.1 km) it is 209 ms. During both disturbances, the angle of 140° was reached in the critical fault time.

The results of the simulations show that the angle of 140° could be used as the trigger criterion for the out of step protection function of the analyzed machine. For some other machine it might be the case that this angle should be lower or even higher. It would be possible to set a lower trigger value (e.g., 120°) and condition the tripping of the generator with the number of slipping cycles. This will ensure that the machine is not tripped unselectively for the power swings in the transmission network. However, it would be better to use load angle values together with some other condition. According to Equation (8), the change of generator speed is proportional to the rate of change of the load angle. The results of the simulation show that the load angle rate of change for unstable power swing, near the critical load angle values, does not change its sign, i.e., it is always positive. On the other hand, when we have stable power swing, the load angle rate of change switches from positive

to negative values near critical load angle values. This behavior implies that the rate of change of the load angle together with the load angle value can be used for the loss of synchronicity fault detection.

5. Conclusions

This article deals with the angle stability problem that occurs on synchronous generators, and how to predict and/or detect this loss of synchronicity using the real time load angle measurement method. The results of the conducted research are presented in the article. The goal was to find out whether a real time load angle measurement which can be used for detecting the generator out of step can be realized.

The real time load angle measurement algorithm was developed and evaluated on a real hydrogenerator in the Dubrava HPP. The capacitive air gap sensor method is used for load angle measurement. The results show that the measurement method and the developed algorithm give very accurate real time load angle measurements with the highest possible resolution. This allows the usage of the load angle in detecting the synchronous generator out of step, which further requires the development of an out of step algorithm or a generator protection function. The development of such an algorithm is the subject of future research. The results of the conducted loss of synchronicity simulations, some of which are presented in Section 4, will be used in the development of the out of step protection algorithm. The here presented results also show that the load angle can be used for detecting the synchronous generator out of step.

Power system stability and in particular rotor angle stability of multimachine power systems should be analyzed taking into account local variables of different nodes in the network. For this reason, further research will focus on the distribution of the load angle measurements via the communication network towards other systems by using standard communication protocols designed for automation and control systems. The intention is to analyze the possibility of using the load angle measurements from generators in the power system for system integrity protection schemes (SIPS) but also to make the load angle available to other systems that could use it for different purposes, but are not able to measure it themselves.

Author Contributions: Conceptualization, I.V. and I.S.; methodology, I.V.; software, I.V. and I.S.; validation, I.V.; formal analysis, I.V.; investigation, I.V. and I.S.; resources, A.M.; data curation, I.S.; writing—original draft preparation, I.V.; writing—review and editing, I.V. and I.S.; visualization, I.S.; supervision, A.M.; project administration, I.V.; funding acquisition, I.V. and I.S. All authors have read and agreed to the published version of the manuscript.

Funding: This project is co-financed by the Croatian Agency for SMEs, Innovations and Investments (HAMAG-BICRO), from the “Proof of Concept” program.

Conflicts of Interest: The authors declare no conflict of interest.

References

1. Machowski, J.; Bialek, J.W.; Bumby, J.R. *Power System Dynamics, Stability and Control*; John Wiley & Sons Ltd.: New Jersey, NJ, USA, 2008.
2. Abedini, M.; Davarpanah, M.; Sanaye-Pasand, M.; Hashemi, S.M.; Irvani, R. Generator Out-of-Step Prediction Based on Faster-Than Real Time Analysis: Concepts and Applications. *IEEE Transactions on Power Systems* **2018**, *33*.
3. Berdy, J. *Out of Step Protection for Generators*. General Electric Power Management: Ontario, ON, Canada. Available online: <https://store.gegridsolutions.com/FAQ/Documents/CEB/GER-3179.pdf> (accessed on 26 April 2020).
4. Cheng, S.; Sachdev, M.S. Out of Step Protection Using the Equal Area Criterion. Proceedings of the 18th Annual Canadian Conference on Electrical and Computer Engineering, Saskatoon, Saskatchewan, Canada, 1-4 May 2005, 1488-1491.
5. Reimert, D. *Protective Relaying for Power Generation Systems*; Taylor & Francis: Abingdon, UK, 2006.
6. Jadrić, M.; Frančić, B. *Dynamics of Electrical Machines*; Graphis: Zagreb, Croatia, 1997.
7. Mišković, M.; Mirošević, M.; Ergec, G. Load Angle Estimation of a Synchronous Generator Using Dynamical Neural Networks. *Journal of Energy* **2009**, *58*, 174-191.

8. Višić, I.; Strnad, I.; Tonković, T. Real Time Load Angle Application for Synchronous Generator Protection Purposes. *Journal of Energy* **2020**, *69*, 13-17.
9. Višić, I.; Strnad, I.; Tonković, T. Real Time Load Angle Application for Synchronous Generator Protection Purposes. Proceedings of the 2nd International Colloquium on Intelligent/Smart Grid Metrology 2019 - SMAGRIMET, Split, Croatia, 9-12 April 2019, 66-70.
10. Kundur, P. *Power System Stability and Control*; McGraw-Hill: New York, NY, USA, 1994.
11. Tziouvaras, D. A.; Hou, D. Out-of-step protection fundamentals and advancements. Proceedings of the 57th Annual Conference for Protective Relay Engineers, College Station, Texas, USA, 1 April 2004, 282-307.
12. Despalatović, M.; Jadrić, M.; Terzić, B. Real-time power angle determination of salient-pole synchronous machine based on air gap measurements. *Electric Power Systems Research* **2008**, *78*, 1873-1880.
13. *Veski Capacitive air gap sensor*. Available online: <https://www.veski.hr/index.php?page=sensors-ag> (accessed on 30 May 2020).
14. *Vibrosystem Air Gap monitoring*. Available online: https://www.vibrosystem.com/en/product/vm_air_gap (accessed on 30 May 2020).
15. *Iris Power Capacitive air gap sensor*. Available online: <https://irispower.com/products/capacitive-air-gap-sensor/> (accessed on 30 May 2020).
16. Orešković, G.; Meško, B. HPP Dubrava – Power Swings and Electromechanical Oscillations of Generator A and B. Expert study, Veski Ltd and Faculty of Electrical Engineering and Computing, Zagreb, Croatia, 2004.
17. Despalatović, M.; Jadrić, M.; Terzić, B.; Macan, J. On-Line Hydrogenerator Power Angle and Synchronous Reactances Determination Based on Air Gap Measurement. Proceedings of the IEEE PES Power Systems Conference and Exposition, New York, NY, USA, 10-13 October 2004, 753-758.
18. Jadrić, M.; Despalatović, M.; Terzić, B.; Rajković, B. Methodology for Synchronous Hydrogenerator Parameter Identification Based on Monitoring System Measurement. *Automatika* **2007**, *48*, 9-19.
19. Lopac, N.; Bulic, N.; Vrkic, N. Sliding Mode Observer-Based Load Angle Estimation for Salient-Pole Wound Rotor Synchronous Generators. *Energies* **2019**, *12*, 1609.
20. *International Guide on the protection of Synchronous Generators*; CIGRE Working Group B5.04.: **2011**, Brochure 479, 122-133.
21. *SIPROTEC 4 Generator Protection 7UM62 Manual*; Siemens AG: Nürnberg, Germany, 2017.
22. Fischer, N.; Benmouyal, G.; Hou, D.; Tziouvaras, D.; Byrne-Finley, J.; Smith, B. Tutorial on Power Swing Blocking and Out-of-Step Tripping. Proceedings of the 39th Annual Western Protective Relay Conference, Spokane, Washington, WA, USA, 16-18 October 2012.
23. Camarillo-Peñaranda, J. R.; Celeita, D.; Gutierrez, M.; Toro M.; Ramos, G. An Approach for Out-of-Step Protection Based on Swing Center Voltage Estimation and Analytic Geometry Parameters. *IEEE Trans. Ind. Appl.* **2020**, *56*, 2402-2408.
24. Redfern, M.A.; Checksfield, M.J. A New Pole Slip Protection Algorithm for Dispersed Storage and Generation using the Equal Area Criterion. *IEEE Transactions on Power Delivery* **1995**, *10*, 194-202.
25. Redfern, M.A.; Checksfield, M.J. A Study into a New Solution for the Problems Experienced with Pole Slipping Protection. *IEEE Transactions on Power Delivery* **1998**, *13*.
26. Kumar, N.; Nagaraja, D.R.; Khincha, H.P. A smart and adaptive scheme for generator out of step protection. Proceedings of the 2015 IEEE Innovative Smart Grid Technologies-Asia (ISGT ASIA), Bangkok, Thailand, 3-6 November 2015.
27. Alinezhad B.; Karegar, H. K. Out-of-Step Protection Based on Equal Area Criterion. *IEEE Transactions on Power Systems* **2017**, *32*, 968-977.
28. Paudyal, S.; Ramakrishna, G.; Sachdev, M.S. Application of Equal Area Criterion conditions in the Time Domain for Out-of-Step Protection. *IEEE Transactions on Power Delivery* **2010**, *25*, 600-609.
29. Haner, J.M.; Laughlin, T.D.; Taylor, C.W. Experience with the RRdot Out of Step Relay. *IEEE Transactions on Power Systems* **1986**, *PWRD-1*, 35-39.
30. Fan, D.; Centeno, V. Adaptive out-of-step protection schemes based on synchrophasors. Proceedings of the IEEE Power & Energy Society General Meeting, Washington, WA, USA, 27-31 July 2014.
31. Sauhats, A.; Utans, A.; Antonovs, D.; Svalovs, A. Angle Control-Based Multi-Terminal Out-of-Step Protection System. *Energies* **2017**, *10*, 308.

32. Orešković, G.; Bacinger, I.; Dvekar, Đ. Active Power Oscillation cause detection in HPP Dubrava applying generator power angle measurement. Proceedings of the 7th HRO CIGRE Session, Cavtat, Croatia, November 2005.
33. Brezovec, M.; Brkljac B.; Kuzle, I. Influence of operating conditions on hydrounit power oscillations. Proceedings of the Eurocon 2013 Conference, Zagreb, Croatia, 1-4 July 2013, 1453-1459.



© 2020 by the authors. Licensee MDPI, Basel, Switzerland. This article is an open access article distributed under the terms and conditions of the Creative Commons Attribution (CC BY) license (<http://creativecommons.org/licenses/by/4.0/>).